850-nm hybrid fiber/free-space optical communications using orbital angular momentum modes

Jurado-Navas, Antonio; Tatarczak, Anna; Lu, Xiaofeng; Vegas Olmos, Juan José; Garrido-Balsellss, José María; Tafur Monroy, Idelfonso

Published in:
Optics Express

Link to article, DOI:
10.1364/OE.23.033721

Publication date:
2015

Document Version
Publisher's PDF, also known as Version of record

850-nm hybrid fiber/free-space optical communications using orbital angular momentum modes

Antonio Jurado-Navas,[1,2,*] Anna Tatarczak,[1] Xiaofeng Lu,[1] Juan José Vegas Olmos,[1] José María Garrido-Balsells,[2] and Idelfonso Tafur Monroy[1]

[1]*Dpt. Photonics Engineering, Technical University of Denmark (DTU), Akademivej Building 358, 2800 Kgs. Lyngby, Denmark*

[2]*2Department of Communications Engineering, University of Málaga, Campus de Teatinos s/n, 29071 Málaga, Spain*

[*]*navas@ic.uma.es*

Abstract: Light beams can carry orbital angular momentum (OAM) associated to the helicity of their phasefronts. These OAM modes can be employed to encode information onto a laser beam for transmitting not only in a fiber link but also in a free-space optical (FSO) one. Regarding this latter scenario, FSO communications are considered as an alternative and promising mean complementing the traditional optical communications in many applications where the use of fiber cable is not justified. This next generation FSO communication systems have attracted much interest recently, and the inclusion of beams carrying OAM modes can be seen as an efficient solution to increase the capacity and the security in the link. In this paper, we discuss an experimental demonstration of a proposal for next generation FSO communication system where a light beam carrying different OAM modes and affected by $\mathscr{M}$ turbulence is coupled to the multimode fiber link. In addition, we report a better and more robust behavior of higher order OAM modes when the intermodal dispersion is dominant in the fiber after exceeding its maximum range of operation.

OCIS codes: (010.1330) Atmospheric turbulence; (290.5930) Scintillation; (060.1155) All-optical networks.

References and links

1. K. Kazaura, K. Wakamori, M. Matsumoto, T. Higashino, K. Tsukamoto, and S. Komaki, "RoFSO: a universal platform for convergence of fiber and free-space optical communication networks," IEEE Commun. Mag. **48**, 130–137 (2010).
2. J. J. Vegas Olmos, X. Pang, A. Lebedev, M. Sales Llopis, and I. Tafur Monroy, "Wireless and wireline service convergence in next generation optical access networks - the FP7 WISCON project," IEICE Trans. Commun. **E97-B**, 1537–1546 (2014).
3. K. Kazaura, K. Omae, T. Suzuki, M. Matsumoto, E. Mutafungwa, T. Murakami, K. Takahashi, H. Matsumoto, K. Wakamori, and Y. Arimoto, "Performance evaluation of next generation free-space optical communication system," IEICE Trans. Electron. **E90-C**, 381–388 (2007).
4. G. Parca, A. Shahpari, V. Carrozzo, G. Tosi Beleffi, and A. J. Teixeira, "Optical wireless transmission at 1.6-tbit/s (16×100 Gbit/s) for next-generation convergent urban infrastructures," Opt. Eng. **52**, 116102 (2013).
5. E. Ciaramella, Y. Arimoto, G. Contestabile, M. Presi, A. D'Errico, V. Guarino, and M. Matsumoto, "1.28 Terabit/s (32×40 Gb/s) WDM transmission over a double-pass free space optical link," IEEE J. Sel. Areas Commun. **27**, 1639–1645 (2009).

#251555 Received 7 Oct 2015; revised 15 Dec 2015; accepted 17 Dec 2015; published 22 Dec 2015

6. G. Nykolak, P.F. Szajowski, D. Romain, G.E. Tourgee, H.M. Presby, and J.J. Auborn, "Update on 4×2.5 Gb/s, 4.4 km free-space optical communications link: availability and scintillation performance," Proc. SPIE **3850**, 11–19 (1999).
7. S. Mi, T. Wang, G. Jin, and C. Wang, "High-capacity quantum secure direct communication with orbital angular momentum of photons," IEEE Photonics J. **7**, 1–8 (2015).
8. I. B. Djordjevic and M. Arabaci, "LDPC-coded orbital angular momentum (OAM) modulation for free-space optical communication," Opt. Express **18**, 24722–24728 (2010).
9. I. B. Djordjevic, "Deep-space and near-Earth optical communications by coded orbital angular momentum (OAM) modulation," Opt. Express **19**, 14277–14289 (2011).
10. A. E. Wilner, H. Huang, Y. Yan, Y. Ren, N. Ahmed, G. Xie, C. Bao, L. Li, Y. Cao, Z. Zhao, J. Wang, M. P. J. Lavery, M. Tur, S. Ramachandran, A. F. Molisch, N. Ashrafi, and S. Ashrafi, "Optical communications using orbital angular momentum beams," Adv. Opt. Photon. **7**, 66–106 (2015).
11. J Wang, J. Y. Yang, I. M. Fazal, N. Ahmed, Y. Yan, H. Huang, Y. Ren, Y. Yue, S. Dolinar, M. Tur, and A. E. Willner, "Terabit free-space data transmission employing orbital angular momentum multiplexing," Nat. Photonics **6**, 488–496 (2012).
12. A. H. Ibrahim, F.S. Roux, M. McLaren, T. Konrad, and A. Forbes, "Orbital-angular-momentum entanglement in turbulence," Phys. Rev. A **88**, 012312 (2013).
13. C. Paterson, "Atmospheric turbulence and orbital angular momentum of single photons for optical communication," Phys. Rev. Lett. **94**, 153901 (2005).
14. M. Mirhosseini, M. Malik, Z. Shi, and R.W. Boyd, "Efficient separation of the orbital angular momentum eigenstates of light," Nat. Commun. **4**, 2781 (2013).
15. M. Krenn, R. Fickler, M. Fink, J. Handsteiner, M. Malik, T. Scheidl, R. Ursin, and A. Zeilinger, "Communication with spatially modulated light through turbulent air across Vienna," http://arxiv.org/abs/1402.2602.
16. H. Refai, J. Sluss, and M. Atiquzzaman, "Comparative study of the performance of analog fiber optic links versus free-space optical links," Opt. Eng. **45**, 025003 (2006).
17. A. Tatarczak, M. A. Usuga, and I. T. Monroy, "OAM-enhanced transmission for multimode short-range links," Proc. SPIE **9390**, 93900E (2015).
18. A. Jurado-Navas, J. M. Garrido-Balsells, J.F. Paris, and A. Puerta-Notario, "A unifying statistical model for atmospheric optical scintillation," in: *Numerical Simulations of Physical and Engineering Processes*, Jan Awrejcewicz, ed. (In-Tech, 2011), pp. 181–206.
19. A. Jurado-Navas, J.M. Garrido-Balsells, J.F. Paris, M. Castillo-Vázquez, and A. Puerta-Notario, "General analytical expressions for the bit error rate of atmospheric optical communication systems: erratum," Opt. Lett. **39**, 5896 (2014).
20. G. Zhao and Y. Zhang, "The effect of tilt aberration and astigmatism of turbulent atmosphere on the intensity distribution of a vortex carrying Gaussian beam," Optik **122**, 29–32 (2011).
21. Draka Industry, http://www.drakausa.com/default.aspx
22. L. C. Andrews, R. L. Phillips, and C.Y. Hopen, *Laser Beam Scintillation with Applications* (Bellingham, 2001).
23. M. A. Al-Habash, L. C. Adrews, and R. L. Phillips, "Mathematical model for the irradiance probability density function of a laser beam propagating through turbulent media," Opt. Eng. **40,** 1554–1562 (2001).
24. J. M. Garrido-Balsells, A. Jurado-Navas, J. F. Paris, M. Castillo-Vázquez, and A. Puerta-Notario, "Novel formulation of the M model through the Generalized-K distribution for atmospheric optical channels," Opt. Express **23**, 6345–6358 (2015).
25. G. Gibson, J. Courtial, and M. J. Padgett, "Free-space information transfer using light beams carrying orbital angular momentum," Opt. Express **12**, 5448–5456 (2004).
26. J. A. Anguita, M. A. Neifeld, and B. V. Vasic, "Turbulence-induced channel crosstalk in an orbital angular momentum-multiplexed free-space optical link," App. Opt. **47**, 2414–2429 (2008).
27. P. T. Dat, A. Bekkali, K. Kazaura, K. Wakamori, T. Suzuki, M. Matsumoto, T. Higashino, K. Tsukamoto, and S. Komaki, "Studies on characterizing the transmission of RF signals over a turbulent FSO link," Opt. Express **17**, 7731–7743 (2009).
28. G. A. Tyler and R. W. Boyd, "Influence of atmospheric turbulence on the propagation of quantum states of light carrying orbital angular momentum," Opt. Lett. **34**, 142–144 (2009).
29. Y. Ren, H. Huang, G. Xie, N. Ahmed, Y. Yan, B. Erkmen, N. Chandrasekaran, M. P. J. Lavery, N. Steinhoff, M. Tur, S. Dolinar, M. Neifeld, M. Padgett, R. W. Boyd, J. Shapiro, and A. E. Wilner, "Atmospheric turbulence effects on the performance of a free space optical link employing orbital angular momentum multiplexing," Opt. Lett. **38**, 4062–4065 (2013).
30. Y. Ren, G. Xie, H. Huang, C. Bao, Y. Yan, N. Ahmed, M. P. J. Lavery, B. I. Erkmen, S. Dolinar, M. Tur, M. A. Neifeld, M. J. Padgett, R. W. Boyd, J. H. Shapiro, and A. E. Willner, "Adaptive optics compensation of multiple orbital angular momentum beams propagating through emulated atmospheric turbulence," Opt. Lett. **39**, 2845–2848 (2014).
31. M. McLaren, T. Mhlanga, M. J. Padgett, F. S. Roux, and A. Forbes, "Self-healing of quantum entanglement after an obstruction," Nat. Commun. **5**, 3248 (2014)
32. B. J. Smith and M. G. Raymer, "Two-photon wave mechanics," Phys. Rev. A **74**, 062104 (2006).

#251555 Received 7 Oct 2015; revised 15 Dec 2015; accepted 17 Dec 2015; published 22 Dec 2015

33. D. L. Fried, "Optical resolution through a randomly inhomogeneous medium for very long and very short exposures," J. Opt. Soc. Am. **56**, 1372–1379 (1966).
34. V. P. Lukin, P. A. Konyaev, and V. A. Sennikov, "Beam spreading of vortex beams propagating in turbulent atmosphere," Appl. Opt. **51**, C84–C87 (2012).
35. A. Jurado-Navas, J.M. Garrido-Balsells, M. Castillo-Vázquez, and A. Puerta-Notario, "An efficient rate-adaptive transmission technique using shortened pulses for atmospheric optical communications," Opt. Express **18**, 17346–17363 (2010).

1. Introduction

In the last few years, free-space optical (FSO) communication systems have attracted considerable research efforts mainly due to their inherent potential transmission capacity, much higher than that offered by radio transmission technologies. Concretely, FSO systems can be applied for metro-access network extension, last mile access, enterprise connectivity and, additionally, it presents interesting applications in the development of trunk links in metropolitan area networks (MAN). Such systems are also used in hybrid radio on free-space optical (RoFSO) or in all-optical hybrid fiber communication systems [1, 2]. Considering their narrow beam widths and its inherent license-free operation as compared with microwave systems, FSO systems are appropriate candidates for secure, high-data-rate, cost-effective, wide-bandwidth communications.

The next-generation FSO systems [1, 3] can provide even a higher data-rate and capacity. Those types of systems are based on transmitting an optical beam over an atmospheric link that, afterwards, it will be directly coupled into an optical fiber core. In particular, we present in this paper a 850 nm hybrid fiber-FSO system as one plausible realisation of this next-generation FSO links, where signal is emitted directly to free space from a fiber termination point, whilst in the receiver side, the light is focused directly into the fiber core. Hence, the need to convert the optical signal from electrical to optical formats or vice versa for transmitting or receiving through the atmospheric medium is removed. As a direct consequence, extremely high data rates of 1 Tb/s and beyond are feasible to achieve [4, 5]. Additionally, it is possible to achieve a higher efficiency in terms of bandwidth when a multimode fiber (MMF) is employed so that the FSO beam can be coupled into it [6].

However, FSO links do not take advantage of the available spectra. In this regard, and thanks to its inherent orthogonality, orbital angular momentum (OAM) of light can mitigate this aspect when multiplexing various information channels, where each mode of light carries different information. Therefore, the inclusion of OAM modes in these systems can increase the level of security [7] and the capacity associated to the FSO link in a remarkable manner [8–10]. The OAM of light beam is the component of angular momentum dependent on the field spatial distribution, and not on the state of polarization, and hence unrelated to the spin of individual photons. Furthermore, those OAM of light beams are called 'vortex beams' with vortex defining an integer number, the topological charge, depending on the number of times the light twists around its axis of travel in one wavelength.

On another note, we can distinguish both an internal and an external OAM. The first one is an origin-independent angular momentum of a light beam associated with a helical or twisted wavefront. Accordingly, the external OAM denotes the origin-dependent angular momentum that can be obtained as the cross product of the light beam position (center of the beam) and its total linear momentum [11]. The OAM modes form an infinite-dimensional Hilbert space so that multiple light beams can coexist within the same space without interfering to each other (OAM beams with different azimuthal OAM states are mutually orthogonal). Consequently, as we said before, that behavior achieves an effective increase in the channel information capacity through higher data transmission rates, constituting a key motivation for including these OAM-carrying pulses in a next-generation FSO system.

#251555 Received 7 Oct 2015; revised 15 Dec 2015; accepted 17 Dec 2015; published 22 Dec 2015

However, turbulence-induced fading introduces a loss of information in the OAM modes, not seen as a pure decoherence process because the information is not transferred to the medium, but to a part of the same Hilbert space since it is scattered into many other different OAM states [12]. Higher-order modes are even more susceptible to this effect [13] as we have checked in this paper. Nevertheless, we report in this manuscript that those higher-order OAM modes present a more robust behavior when the intermodal dispersion is dominant in the fiber, i.e., after exceeding the maximum distance (300 m in our case) required for a 10 Gigabit Ethernet transmission can be run. We must say we are not transmitting a superposition of OAM modes but different OAM modes in separated transmissions. For the first case, we would be required to distinguish those modes with different techniques as for instance, holograms [14] or, more recently, directly observing the unambiguous mode-intensity pattern and using a pattern recognition algorithm to that end [15]. In our case, we consider OAM modes of orders 1 to 3 independently transmitted with the purpose of providing its performance through a all-optical system for different turbulence regimes and, additionally, to report the higher robustness shown by higher-order OAM modes in the intermodal dispersion range.

2. Hybrid fiber-FSO communication link operating at 850 nm

Hybrid fiber-FSO communication systems has been developed to overcome some limitations presented in conventional FSO systems as, for instance, the necessity of converting the signal from electrical to optical formats or vice versa for transmitting or receiving through the atmosphere. An all-optical hybrid fiber-FSO system is represented in Fig. 1.

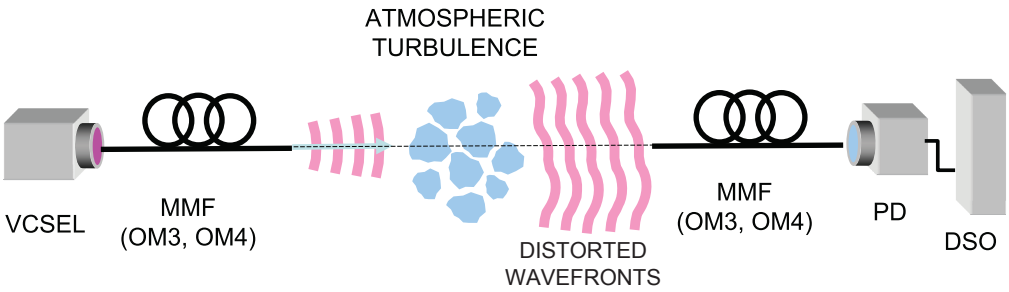

Fig. 1. Principle of a hybrid fiber-FSO system. Beams emitted by the vertical cavity surface-emitting laser (VCSEL) are directly coupled into a multimode fiber (MMF) and transmitted through the atmospheric channel. The distorted beam is then focused directly on the core of a new optical fiber, and the optical signal propagates to the proper detector (a photodiode, PD, in this case). Finally, the data is stored at digital storage oscilloscope (DSO).

There, the optical signal is emitted by a vertical cavity surface-emitting laser (VCSEL) and guided by an optical multimode fiber (MMF) to collimating optics. In this paper, the VCSEL is operating at 850 nm. From a market point of view, that wavelength of 850 nm is a wavelength standardized for short range communication purposes. After that, the optical beam is directly transmitted to an atmospheric channel from the fiber termination point. The atmosphere will distort the optical wavefront with more or less impact depending on the intensity of the turbulence. In the receiver side, the received optical beam is directly focused on the core of a second MMF.

As it is straightforward to see, those types of systems are based on transmitting an optical beam over an atmospheric link that, afterwards, will be directly coupled into an optical fiber core. Hence, unlike conventional FSO systems, these hybrid fiber-FSO communication links do not require costly electro-optical and opto-electrical converters neither additional amplifications

#251555 Received 7 Oct 2015; revised 15 Dec 2015; accepted 17 Dec 2015; published 22 Dec 2015

stages before transmitting or receiving through the atmospheric channel.

Thus, in the receiver side, the received optical signal propagates down the MMF to the detector, in our case, a 850 nm commercially available photodiode (PD) since a direct detection procedure is implemented. Finally, the signal is then stored at digital storage oscilloscope (DSO) for further analysis.

We can indicate several advantages associated to these hybrid fiber-FSO systems. First, it is a robust low-cost technology due to the fact that no electro-optical or opto-electrical conversion processes are required. Second, its inherent simplicity providing fast deployments. And third, transceivers are not required to be placed together with other electronics in one main unit, but they can be located remotely.

One of the objectives associated to this hybrid fiber-FSO technologies is to establish communications using the 10 Gigabit Ethernet (GbE) standard, mostly applied in Local Area Networks (LAN). Among the attractive applications involving these systems, we can remark their use to extend broadband connectivity to under-served areas, but also they can be employed for metro network extension, last mile access, enterprise connectivity, access technology for providing broadband heterogeneous wireless services, or as an extension of Radio over Fiber into atmospheric links [16].

3. Experimental setup

We present here a system using on-off keying (OOK) intensity modulation over a combined atmospheric channel – multimode fiber measured for various OAM modes. To keep the system complexity low, direct detection was used [8] just after the information was propagated through both the FSO link and the MMF. In this regard, our experiment employs those pulses transporting OAM modes to increase the capacity or the reach without requiring to utilize mode division multiplexing (MDM) in the fiber side and, accordingly, without increasing the complexity in

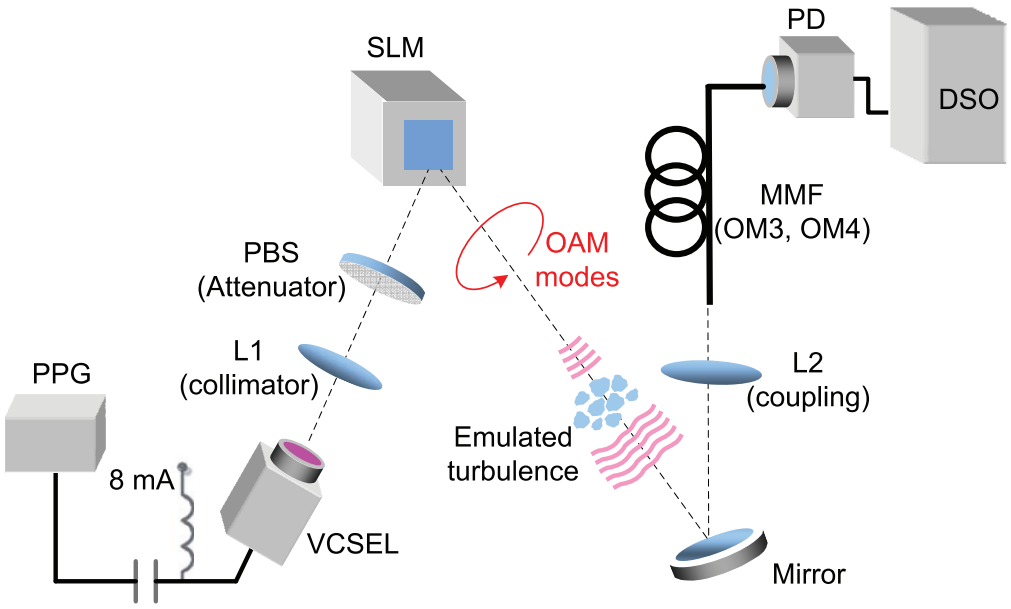

Fig. 2. Experimental setup for the transmission of beams carrying OAM modes over MMF. The signal coupled into the fiber will be affected by turbulence generated by computer in order to emulate the effect of the turbulence atmosphere.

#251555 Received 7 Oct 2015; revised 15 Dec 2015; accepted 17 Dec 2015; published 22 Dec 2015

the system.

Figure 2 shows the experimental setup implemented in this paper. First of all we have the vertical cavity surface emitting laser (VCSEL) operating at 850 nm since these types of lasers are widely extended due to their low power consumption and its inherent small footprint. The laser is biased at 8 mA and directly modulated with a pseudo-random bit sequence of $2^{15} - 1$ samples generated by a pulse pattern generator (PPG) at two different rates: 10 Gbps or 11 Gbps [17]. The choice of those bit-rates are coincident with the 10 Gb/s Ethernet without and with forward error correction (FEC), respectively. Nevertheless, the main purpose in this experiment is to research the performance associated to analog signal transmission over OAM in FSO-MMF links.

Then the modulated optical beam is transmitted to free-space and collimated when passing through lens L1. The frequency response of the optical channel implemented in this work is described in more detail in [17]. After that, and still in free-space, the polarization beam splitter (PBS) acts as a controllable variable attenuator so that we can obtain different bit error rate curves by directly varying the level of the transmitted power. Then, the resulting beam light passes through a half-wave plate which shifts the polarization direction of the beam. At this point we have a linearly polarized Gaussian beam. Then, the optical beam reaches the spatial light modulator (SLM). The SLM is used to form the OAM modes. We must remark that the combination of VCSEL and OM4 (and also OM3) multimode fiber is the typical core of the short-range links widely used in commercial data center infrastructures.

Next, the signal is directly coupled to a MMF OM3 fiber standard patch cord 3 meter long, ensuring that a perfect alignment was achieved to obtain a maximum level of received power, requiring a readjust for each of the OAM modes transmitted. Hence, the free-space section is completed at this point. The full length of that free-space link is fixed to 1.5 meters but we vary the pattern of the received intensity in the MMF patch cord by generating different computer-assisted turbulence regimes. Accordingly, a sequence of normalized scintillation following a Málaga distribution [18, 19] was employed to model those different turbulence intensities from a very weak one up to a moderate turbulence regime in a manner similar to [20].

At this point we illustrate the resulting distorted modes M0 to M3 that were captured with the camera and displayed in Fig. 3 for a very weak turbulence. Due to the existence of a phase singularity of OAM modes, there is no intensity at their centers (Fig. 3(b)–3(d)). In addition, some particles of dust in the camera under the glass at the top of the lens can be also distinguished in that Fig. 3.

Next the OM3 patch cord that was employed to couple the signal from the free-space link is then connected to a multimode fiber spool using for this purpose the fiber connector. In this paper, two different multimode fiber standards were utilized: a 100-meter OM3 in addition to a 400-meter OM4 special fiber (Max-CAP-OM4) manufactured by Draka [21]. Their respective losses are below 0.5 dB for the OM3 and 0.97 for the Draka OM4.

Finally, the signal transmitted through the fiber link is captured by a 850 nm photodiode with 25 GHz bandwidth and recorded at a digital oscilloscope with 14 GHz bandwidth.

3.1. Prospects for a real FSO reach

In a future, we are planning to implement a real link covering the distance between Building 358 and Building 403, both in the DTU Lyngby Campus, as indicated in Fig. 4. Such a distance is 423 m. Hence, with this perspective in mind, we included a turbulence generated by computer in the experimental setup described above, where it was assumed that propagation path length of 423 m. Then, four turbulent scenarios were established: very weak, weak, weak-to-medium and moderate turbulence. Table 1 summarizes the values characterizing each turbulence regime, following a Málaga propagation model [18, 19].

#251555 Received 7 Oct 2015; revised 15 Dec 2015; accepted 17 Dec 2015; published 22 Dec 2015

Table 1. **Generation of different turbulence regimes from the $\mathscr{M}$ distribution model.**

Turbulence regime	σ_I^2	C_n^2 $(\times 10^{-15})$	Ω	ρ	α	β
Very Weak	0.01	1.81	0.98	0.98	143	140
Weak	0.04	4.82	0.9	0.877	140	120
Weak-to medium	0.1	12	0.833	0.82	50	49
Moderate	0.406	48.96	0.8	0.75	10	5

In Table 1, σ_I^2 represents the scintillation variance, with C_n^2 being the atmospheric refractive-index structure parameter [22], with Ω, ρ, α and β denoting the inherent parameters of the Málaga or $\mathscr{M}$ distribution [18]. Thus Ω is the line-of-sight (LOS) average optical power whereas the ρ denotes the amount of scattering power coupled to the LOS component. In addition, α is a positive parameter related to the effective number of large-scale cells of the scattering process [23]; and β is associated to the total effective small-scale cells. When $\beta \in \mathbb{N}$, the $\mathscr{M}$ model can be physically interpreted as the superposition of β optical sub-channels cor-

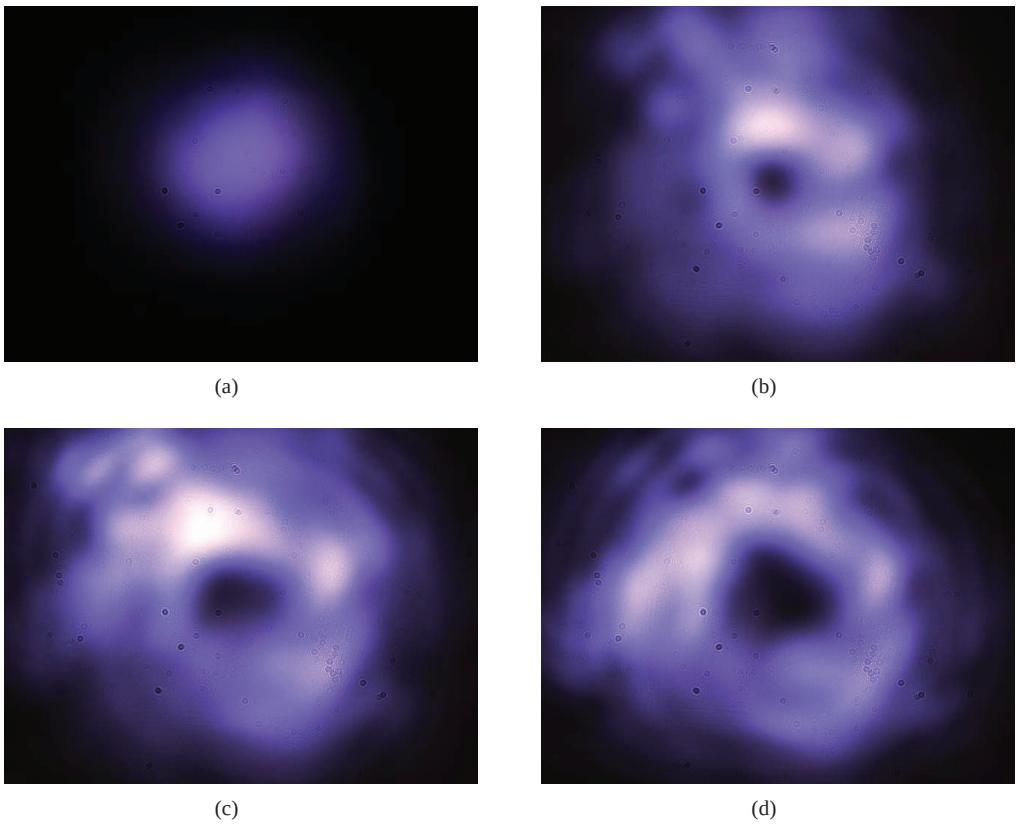

(a) (b) (c) (d)

Fig. 3. Different orbital angular momentum modes captured with the camera after the beam light was affected by the SLM and distorted by a very weak turbulence: (a) mode M0, (b) M1, (c) M2, (d) M3.

#251555 Received 7 Oct 2015; revised 15 Dec 2015; accepted 17 Dec 2015; published 22 Dec 2015

responding, each one, to a different physical optical path, as detailed in [24].

As a remarkable comment, and although any OAM mode is strongly axis-dependent, the effect of misalignment fading on the transmitted pulses [25] is not considered here for the sake of simplicity. That assumption is justified since misalignment has an impact similar to that of weak turbulence, as indicated in [26], this latter effect being completely modeled in our emulated FSO link. In this regard, we can state that all the conclusions we derive through this paper are maintained in a real link. Moreover, and for the sake of clarity, we have not included the effect of rain, fog or snow in our emulated atmospheric channel. Although these hydrometeors affect the transmission of optical beams and limit the maximum range of the link, nevertheless their effect is seen as a deterministic attenuation of the optical wave that can be to some extent solved by increasing transmitting power or using amplifiers [27].

4. Results and discussions

Figures 5-7 shows the behavior of the system in terms of bit error rate (BER) for the different turbulent conditions indicated in Table 1, and for three different types of fiber: first, a transmission over 1 meter (m) of OM3 MMF that, in this paper, we denote as back to back (B2B) transmission, is shown in Fig. 5; second, a transmission over a 100 m OM3, displayed in Fig. 6; and third, a transmission over a OM4 Draka fiber with a length of 400 m, represented in Fig. 7. During the measurement the coupling from the free-space through the L2 is realigned for each mode to reach the highest coupling efficiency. As an important feature, those three figures of results (Figs. 5-7) were built by recording 10^7 symbols per BER point. Afterwards, errors are counted.

For the case of both B2B and 100 m OM3 represented in Figs. 5 and 6, we measured a 3-dB bandwidth of the system of 22 and 18 GHz, respectively, as shown in [17]. Since the

Fig. 4. Distance between Building 358 and Building 403 at Lyngby Campus, Denmark Technical University.

#251555 Received 7 Oct 2015; revised 15 Dec 2015; accepted 17 Dec 2015; published 22 Dec 2015

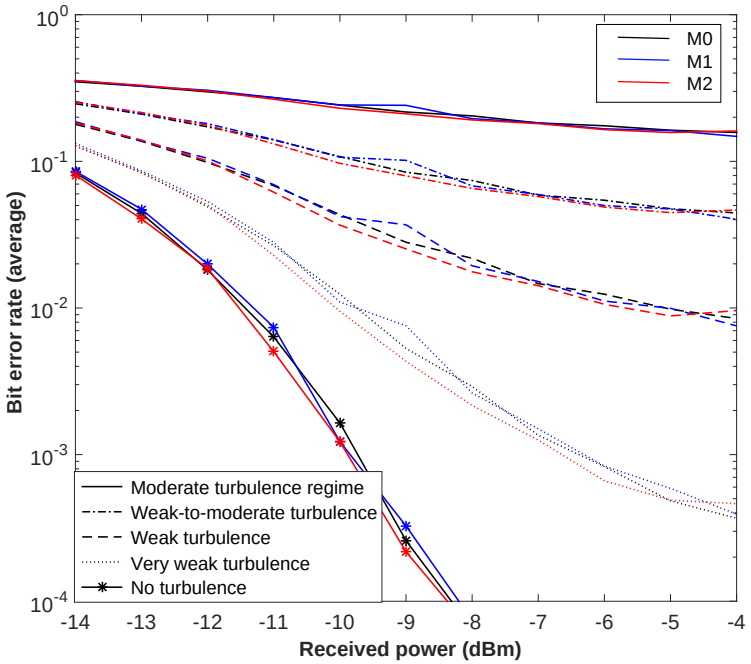

Fig. 5. Bit error rate (BER) versus received optical power measured for back to back and two OAM modes: M1 and M2. Conventional multimode M0 is provided as a reference.

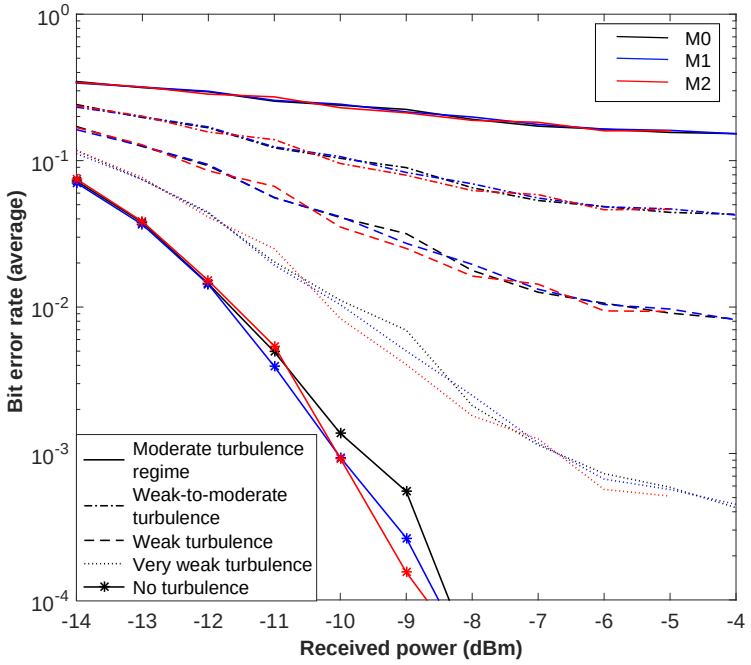

Fig. 6. Bit error rate (BER) versus received optical power measured for 100m OM3 MMF and two OAM modes: M1 and M2. Conventional multimode M0 is provided as a reference.

#251555 Received 7 Oct 2015; revised 15 Dec 2015; accepted 17 Dec 2015; published 22 Dec 2015

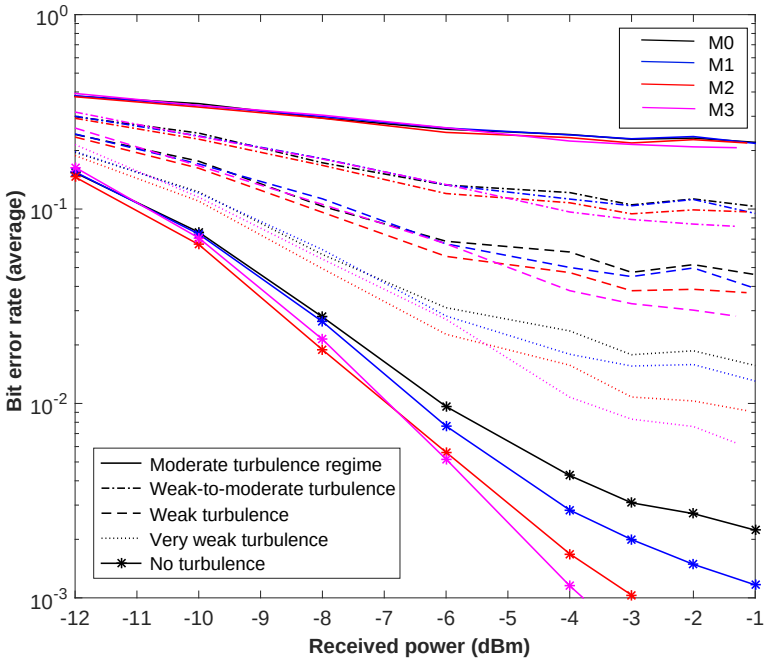

Fig. 7. Bit error rate versus received optical power measured for 400m OM4 Draka MMF and three OAM modes: M1, M2 and M3. Conventional multimode M0 is given as a reference.

transmission rate was established at 11 Gbps in both cases, the aforementioned bandwidths are sufficient for ensuring a transmission without remarkable penalty. Nevertheless, we can observe almost the same behavior in both B2B and 100 m OM3 cases for all the turbulence regimes under study. The reason is simple to understand: no intersymbol interference is produced for this system operating at 11 Gbps through a solely 100 m-length OM3 fiber (the B2B case is, certainly, even more benevolent), still far away from its maximum range (around 300 m) of operation. Thus, the system is not limited by the length of the MMF at all. Considering that we had generated pure Laguerre-Gaussian vortex beam [13] with uniform amplitude within the transmitting aperture and characterized by having helical phase fronts with a phase singularity at their center, then we can assume that the transmitted field can be written, from [28] as:

$$A(\mathbf{r}) = A_0 W\left(\frac{r}{R}\right)\exp(jm\theta), \tag{1}$$

with A_0 representing the field amplitude, with $W(x)$ denoting the aperture function, with R being the radius of aperture, whereas r and θ are the radial and azimuthal coordinates and m is the OAM quantum number. It is straightforward to check that, since the information of the OAM mode is included in the azimuthal phase of the complex electric field, then the irradiance, calculated as $I = |A(\mathbf{r})|^2$, is not affected by m. Results shown in Figs. 5 and 6 verify this fact because it is obtained identical behavior for modes M0, M1 and M2 and a same turbulence regime, analogous to the results showed by Djordjevic [9] in his Fig. 7 for direct detection.

Furthermore, we can notify an important degradation of the system when the atmospheric channel presents a turbulent behavior different to the ideal situation of free-space propagation. For instance, a degradation of 3.2 dBm in the received power is observed for a BER of 10^{-3} when comparing the case of very weak turbulence with respect to the ideal case of no turbu-

#251555 Received 7 Oct 2015; revised 15 Dec 2015; accepted 17 Dec 2015; published 22 Dec 2015

lence. That feature is completely aligned with the results shown in (Fig.6(a) and [[29]], where a single OAM mode was solely transmitted. And the worsening is more pronounced when the intensity of the turbulence increases. Concretely, direct detection schemes can operate properly in weak turbulence regime, while in strong turbulence regime they exhibit error floor phenomena [9] that can be solved by using coherent detection schemes or adaptive optics [30].

On another note, the case displayed in Fig. 7 is completely different. There, a MMF OM4 link of 400 m was used in which the intermodal dispersion is dominant as the limit length of the fiber to guarantee the highest quality in the transmission was exceeded. The measured 3-dB bandwidth was reduced to solely 4.9 GHz [17]. Its associated impact is a loss in the received power of, at least, 2 dB, even although we have realigned all the transmitted modes so that we can reach the highest coupled power.

Notwithstanding, although the system bandwidth is seen as a limiting factor, the inclusion of OAM with higher order modes introduces the most remarkable improvement in the BER performance. For instance, for a same received power of -4 dBm, the corresponding BERs for the modes M0 - M3 are, respectively, $1.15\cdot10^{-3}$, $1.68\cdot10^{-3}$, $2.8\cdot10^{-3}$, $4.26\cdot10^{-3}$ for the ideal case of no turbulence in the link. However, for the case of $\sigma_I^2 = 0.01$, the associated measured BER are 10^{-2}, $1.5\cdot10^{-2}$, $1.79\cdot10^{-2}$ and $2.3\cdot10^{-2}$, respectively for the modes M0 - M3.

Hence, an increasingly improved performance can be apparently observed by shifting vortex modes to higher order, compared to the Gaussian mode M0 when the fiber links are approaching to the dispersion limits. We can assume that it results from higher tolerance of vortex modes to modal dispersion in MMF, with such analysis being part of our future work. Light with Gaussian mode seems to lose power faster by transferring power to side modes and being interfered later by modal dispersion [10]. Yet, such effects of higher order vortex with minimum level of power in its center and spiral energy distribution are not as obvious as the former one, which makes the higher order vortex modes more resistant. This might explain why the performance in shorter fibers is approximately the same, but remarkable different in longer links.

Moreover, the concurrence of the state in OAM modes must be taken into account [31]. Concurrence is, in fact, a measure of the quantum entanglement although in a fragile manner since photons are weakly interacting. For the case of no atmospheric turbulence, it is observed from Fig. 7 that modes with higher OAM retain their entanglement for longer distances than those with lower OAM, verifying the conclusion derived in [32].

However, when atmospheric link is included in the system, the beam waist of the beam must be considered. Higher order OAM modes will present a better robustness regarding their entanglement if the beam waist is much smaller than the turbulence coherence length given by the Fried parameter [33]. Fried parameter, r_0 can be expressed as:

$$r_0 = (0.16C_n^2k^2L)^{-3/5}, \tag{2}$$

as shown in [22], with C_n^2 being the atmospheric refractive-index structure parameter, with k being the wave number of the beam wave, whereas L denotes the propagation path length. It is straightforward to see that for the case of no turbulence, C_n^2 tends to 0 and, accordingly, $r_0 \to \infty$. For that particular case, the beam waist associated to the transmitted light is always much smaller than the Fried parameter and, according to [32], since higher OAM modes retain their entanglement better than lower OAM modes for longer distances, then the case of no turbulence shown in Fig. 7 is justified, as indicated above.

However, since that condition is not valid in general when beam waves are propagated through a turbulent atmospheric medium, then the resulting effect is that higher-order mode beams can be more susceptible to scintillation due to their wider intensity distributions [13], the same effect that we are reporting in Fig. 7. Thus, for instance, in the case of moderate turbulence

#251555 Received 7 Oct 2015; revised 15 Dec 2015; accepted 17 Dec 2015; published 22 Dec 2015

($\sigma_I^2 = 0.406$), behaviors associated to each mode are almost the same whereas, for the case of very weak turbulence (($\sigma_I^2 = 0.01$), a remarkable improvement in BER is reported (around 4 dBm between OAM M3 and OAM M0 for an error probability of $2 \cdot 10^{-2}$), as a direct consequence of a faster divergence, a larger delay and a beam spreading [34] suffered by higher-order OAM modes. Consequently, although all OAM modes are subjected to increased attenuation with increased turbulence strength, however higher-order modes are more strongly affected, being also consistent with Anguita's work [26]. Concretely in that work, and for a propagation path of 1 km, it was studied the existence of a turbulence-induced channel crosstalk. In particular, crosstalk is modeled as an independent Gaussian noise source that adds to the receiver noise, verifying that among OAM modes increases with increased turbulence strength, and with its effect becoming more relevant for higher OAM modes. This effect is completely consistent with the explanation detailed here and, consequently, it is enhanced when OAM modes have suffered some intermodal dispersion range, as it is shown in Fig. 7.

5. Concluding remarks

As a final conclusion, we have experimentally confirmed that the transmission of beams carrying OAM modes are very sensible to the presence of atmospheric turbulence, as presented on Figs. 5–7 even though the system bandwidth is not considered as a limiting factor (Figs. 5 and 6).

In addition, higher order modes are more robust to mitigate the degradation introduced by the system in terms of bandwidth of the system when the operating mode of the MMF is exceeding the dispersion limit length, as shown in Fig. 7. As we commented above, beams carrying higher-order OAM modes are able to retain their entanglement for longer distances confirming the conclusion derived in [32]. From our results, we expect better BER curves for modes M4 – M6 in that particular scenario, being an attractive alternative to mitigate imperfections and microfolds in the fiber. Nevertheless, the presence of the turbulence tends to equalize those differences in behavior. In this respect, the inclusion of adaptive optics, coherent detectors [8, 9], or efficient coding techniques and memory [35] allowing to transmit narrower pulses can compensate the degradation induced by the composed atmospheric-fiber channel.

Acknowledgments

This work was supported by the Andalucía Talent Hub Program launched by the Andalusian Knowledge Agency, co-funded by the European Union's Seventh Framework Program, Marie Skłodowska-Curie actions (COFUND - Grant Agreement no 291780), the HOT project of Danish Innovation Fund, the Marie Curie FENDOI project and the Ministry of Economy, Innovation, Science and Employment of the Junta de Andalucía; and by the Spanish Ministerio de Economía y Competitividad, Project TEC2012-36737.

#251555 Received 7 Oct 2015; revised 15 Dec 2015; accepted 17 Dec 2015; published 22 Dec 2015